



Tannic acid adsorption/desorption study onto/from commercial activated carbon

Shubhjeet Singh, Jai Prakash Kushwaha*

Department of Chemical Engineering, Thapar University, Patiala, Punjab, India
Tel. +91 175 2393388; Fax: +91 175 2393005; email: jps_kag@yahoo.co.in

Received 17 March 2013; Accepted 22 April 2013

ABSTRACT

This study reports tannic acid adsorption onto commercial activated carbon (ACC) in a batch system. Adsorption process parameters namely *pH*, adsorbent dose (m_{ad}), temperature (*T*), initial tannic acid concentration (C_o), and contact time (*t*) were studied and optimized. Optimum *pH* and adsorbent dose were found to be 3.0 and 15 g/l, respectively. Equilibrium contact time was found to be 7 h. Pseudo-second-order kinetic best fits the adsorption kinetic data. Three isotherms namely Langmuir, Temkin, and Redlich and Peterson (R–P) isotherms were studied and it was found that Langmuir and R–P isotherm generally fitted the experimental equilibrium adsorption data. Endothermic nature of the adsorption of tannic acid onto ACC was concluded, and heat of adsorption was found to be as 89.55 kJ/mol. On considering the cost of ACC, regeneration studies of Tannic acid (TA) loaded ACC have been performed using solvent and thermal desorption methods.

Keywords: Tannic acid; Commercial activated carbon; Adsorption kinetics; Isotherms; Regeneration

1. Introduction

Tannic acid (TA) is a phytic substance and occurs naturally in surface and ground water from the breakdown of plant biomass [1]. Also, it is found in industrial wastewater released from coir and cork process, plant medicine, paper, and leather industries [2]. To get better wash fastness properties of acid dyed polyamide, TA is used as after treatment agent. It is also used as a substitute for fluorocarbon after the treatments to impart anti-staining properties to polyamide yarn/carpets. But, a very fastidious and distinctive application of tannic acid in textile is as antistatic agent.

Trihalomethane, a disinfection byproduct that can form in presence of TA during chlorination process for drinking water production which is carcinogenic and can produce liver, kidney, or central nervous system complications [3,4]. Being a water soluble polyphenolic/humic compound, tannic acid has toxicity for aquatic organisms such as algae, phytoplankton, fish, and invertebrates [1]. Therefore, removal of TA from water/wastewater is of great importance in terms of protecting human health and environment.

Biological methods [5] and various physico-chemical treatment methods such as chemical oxidation, electrochemical process, coagulation [6], and nanofiltration (NF) [7] are used to remove TA from water/wastewater. Although biological methods circumvent

*Corresponding author.

using chemicals, but are capable of removing only 30–50% dissolved organic matter from water/wastewater [7] and are energy intensive, demanding much controlling operating conditions [8]. Due to fouling membrane severely, NF has limited TA removal and is very expensive.

Adsorption treatment processes are very efficient for removal of dissolved organic compounds from water/wastewaters with simple operational conditions. Few studies have been reported for the adsorptive removal of TA [1–4,6,7,9–15]. Table 1 shows a comparative assessment of the work reported in the literature. Among these studies, only three studies report TA adsorption on to ACC [11,13,14].

Moreno–Castilla et al. [11] conducted batch and column adsorption study for the removal of herbicide fluroxypyr and TA, using ACC commercial and ACC

cloth. In this study [11], 4 mg/l of TA concentration was used, but in industrial wastewater TA concentration is very high. Moreover, detailed pH effect, kinetic study, thermodynamics, and mechanism of adsorption of TA are lacking.

Sarıcı–Özdemir and Yunus Önal [13] used ACC based on polymeric waste. Equilibration, isotherms, and kinetics has been studied and reported, however, the effect of temperature on thermodynamic parameters was not reported. Regeneration study of adsorbent is also lacking, which is very essential considering the highcost of adsorbent.

Liu et al. [14] studied TA and phenol adsorption on ordered mesoporous carbon (CMK-3) prepared with mesoporous silica SBA-15 template and sucrose as carbon precursor, and post activated with CO₂, coal-based ACC and nonporous pure graphite. Effect

Table 1
Various adsorption studies of tannic acid

Adsorbate	Adsorbent	Optimum condition/kinetic model/isotherms	Reference
Tannic acid	Surfactant-modified zeolites with loadings of cetylpyridinium bromide	pH = 4.0–7.0; pseudo-second-order; Langmuir, R-P, and Silps isotherms	[6]
Tannic acid	Amino functionalized magnetic nanoadsorbent	pH = 6.0; pseudo-second-order; Langmuir isotherms	[2]
Tannic acid	Amino functionalized magnetic mesoporous silica	pH = 6.0, 25°C; pseudo-second-order Langmuir isotherms	[4]
Tannic acid	Commercial resins Xad-7 and D-201	Freundlich isotherms	[7]
Tannic acid and Gallic acid	Bi-function resin WJN-09	Pseudo-first-order and pseudo-second-order; Freundlich	[3]
Tannic acid	Chitosan-montmorillonite	pH = 4.0; Freundlich isotherms	[1]
Tannic acid, Humic acid and dyes	Composite of chitosan and activated clay	Pseudo-first-order; Freundlich isotherms	[9]
Tannic acid	Zirconium pillared clay	pH = 4.0–6.0; first-order reversible reaction; Langmuir and Freundlich isotherms	[10]
Herbicide fluroxypyr and Tannic acid	Activated carbon commercial and activated carbon cloth	Langmuir isotherms	[11]
Tannic acid	Cationic surfactant-modified bentonite clay	pH = 3.0; pseudo-first-order; Langmuir and Freundlich isotherms	[12]
Tannic acid	Activated carbon based on textural waste	Pseudo second-order kinetic model, Langmuir and Freundlich isotherms.	[13]
Tannic acid and phenol	Ordered mesoporous carbon (CMK-3) with mesoporous silica SBA-15 template and sucrose as carbon precursor and activated with CO ₂	Pseudo-second-order kinetic model, Freundlich isotherm	[14]
Tannic acid	Leacril fibre	First-order kinetic	[15]

of concentration of TA on kinetic parameters, and effect of temperature on various isotherm parameters were not reported. Moreover, thermodynamics and regeneration study of adsorbents is completely lacking.

This paper reports the adsorption of TA from aqueous solution onto commercial ACC. The effect of initial pH (pH_i) of the TA solution ($2 \leq \text{pH}_i \leq 10$), adsorbent dose (m_{ad}) ($5 \leq m_{\text{ad}} \leq 25 \text{ g/l}$), contact time (t) ($0 \leq t \leq 7 \text{ h}$), initial TA concentration ($50 \leq C_0 \leq 200 \text{ mg/l}$), and temperature (T) ($291 \leq T \leq 311 \text{ K}$) on the sorption of TA onto ACC has investigated. Kinetics of adsorption and equilibrium characteristics has also been studied. Weber and Morris intraparticle diffusion model were employed to explore the adsorption mechanism. Two and three parameters equilibrium isotherms such as Langmuir, Temkin, and Redlich–Peterson (R–P) isotherms have been examined for their suitability to signify the experimental adsorption data; and isotherm parameters at different temperature were evaluated. Thermodynamic study was also performed to understand the effect of temperature on the TA sorption; and change in Gibbs energy (ΔG_0), entropy (ΔS_0), and enthalpy (ΔH_0) were determined at various temperature. In view of cost of ACC, regeneration studies of TA loaded ACC have been carried out using solvent and thermal desorption methods.

2. Materials and methods

2.1. Adsorbent and TA solution

Coconut-based ACC was supplied by Pneumatic Engineers Spares & Service, New Delhi, India. It was used as procured, except for the removal of very fine particles by sieving. TA was supplied by Merck, Mumbai, India. All the chemicals used were of analytical reagent grade. TA stock solution of 1.0 g/l concentration was prepared by dissolving TA with distilled water and it was diluted in distilled water as per requirement of the experiments.

2.2. Instrumentation

ACC BET surface area was estimated by the standard adsorption of N_2 at 77.15 K by using the Micromeritics ASAP 2020 surface area and porosity analyzer. X' Pert PRO (PANalytical, Philips, Netherlands) with copper as the target was used for XRD analysis. K-Alpha was maintained constant at 1.54060 \AA . Fourier Transform Infrared (FTIR) spectra were obtained in range of $4,000\text{--}400 \text{ cm}^{-1}$ with FTIR spectrometer (Perkin–Elmer, Shimadzu, Japan, model 2000) using KBr pellet technique. The determination

of the concentration of TA prior and after adsorption was performed by finding the absorbance at the characteristic wavelength using a double beam UV-vis spectrophotometer (Perkin–Elmer, Shimadzu, Japan). The wavelength corresponding to maximum absorbance (λ_{max}) was found to be 283 nm .

2.3. Experimental

For batch adsorption study, 250 ml stoppered conical flasks containing a known amount of ACC (g/l) and 100 ml of TA solution of known concentration and pH were taken. Initial pH of the solutions was adjusted by using H_2SO_4 and NaOH solutions. The flasks were transferred into a temperature controlled orbital shaker and the mixture was agitated at a constant speed of 150 rpm at a pre-decided temperature for 7 h to attain equilibrium.

The adsorbent and adsorbate was separated from the mixture after 7 h by filtration with whatman No. 1 filter paper and filtrate was analyzed for residual TA concentration. The percentage removal of TA was calculated using the following relation:

$$\text{Percent removal} = \frac{(C_0 - C_e)100}{C_0} \quad (1)$$

Similarly, equilibrium adsorption uptake, q_e (mg/g) was calculated as:

$$q_e = \frac{(C_0 - C_e)V}{m_{\text{ad}}} \quad (2)$$

where C_e is the equilibrium adsorbate concentration, V is the volume of the adsorbate (l), and m_{ad} is the mass of adsorbent (g).

3. Results and discussion

3.1. Characterization of adsorbent

Pore size distribution is shown in Fig. 1. Pore sizes are classified as micro-pores (diameter (d) $< 20 \text{ \AA}$), meso-pores ($20 \text{ \AA} < d < 500 \text{ \AA}$), and macro-pores ($d > 500 \text{ \AA}$) accordingly with the classification of IUPAC [16]. Micro-pores are further divided into ultra micro-pores ($d < 7 \text{ \AA}$) and super micro-pores ($7 \text{ \AA} < d < 20 \text{ \AA}$). For adsorption of larger sizes of liquid molecules, the adsorbents should be mainly mesoporous in the structure. The BET surface area of ACC was found to be $222.33 \text{ m}^2/\text{g}$, whereas the BET average pore diameter was found to be 26.56 \AA . Therefore, ACC has meso-porous nature which is desirable for adsorption of high weight molecules like TA.

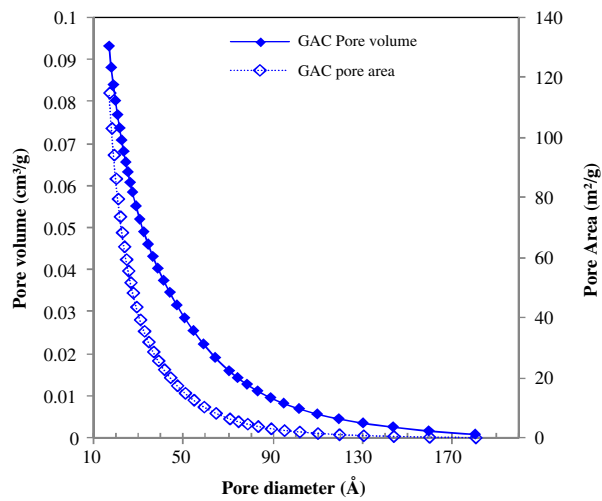


Fig. 1. Pore size distribution of ACC.

XRD spectra of ACC (Fig. 2) showed the presence of Moganite (SiO_2), Tamarugite [$\text{NaAl}(\text{SO}_4)_2 \cdot 6\text{H}_2\text{O}$], Fersilicite (FeSi), and Siderazot (Fe_5N_2) as the chief components. The broader peak in the XRD spectra shows the presence of amorphous form of silica [17].

3.2. Effect of solution initial pH and adsorbent dosage (m_{ad})

Fig. 3 shows the effect of pH_i on the TA removal from aqueous solution by ACC at $T=301\text{ K}$, $t=7\text{ h}$, $C_o=100\text{ mg/l}$, and adsorbent dosage (m_{ad}) = 20 g/l . Highest TA removal efficiency of 67.5 and 66.02% were obtained at $pH_i=2$ and 3, respectively. For all $3 < pH_i \leq 5$, very sharp decrease in TA removal

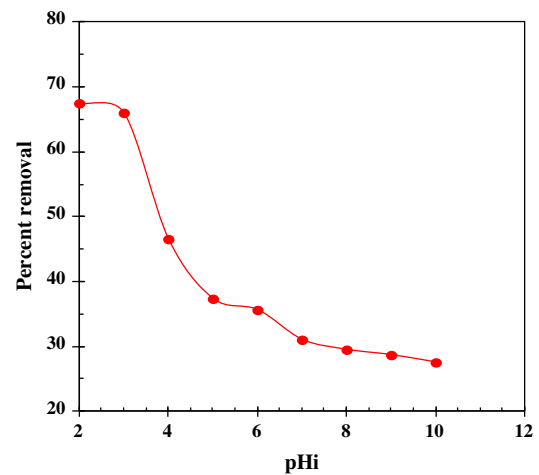


Fig. 3. Effect of pH_i on the TA removal by ACC ($T=301\text{ K}$, $t=7\text{ h}$, $C_o=100\text{ mg/l}$, and $m_{\text{ad-opt}}=20\text{ g/l}$).

efficiency was found. But, for all $pH_i > 5$, TA removal efficiency varied from 35.63 to 27.54%.

TA molecules present in its molecular form at solution $pH \leq 4.5$. TA molecules are dissociated for $pH > 4.5$ and completely ionized at $pH=7$ [1]. Therefore, there is higher removal efficiency for unionized TA at $pH_i \leq 3$ [6]. At higher pH values, the dissociation degree of TA increases leading to the decrease of TA removal efficiency in ACC. It also seems that, at higher pH higher OH^- ions concentration in the solution, compete with TA adsorption onto the ACC, which reduces the TA adsorption. There is no significant differences in the TA removal at $pH_i=2$ and 3, therefore, $pH_i=3$ was chosen as optimum pH_i ($pH_{i\text{-opt}}$) to save the acid used for pH adjustment.

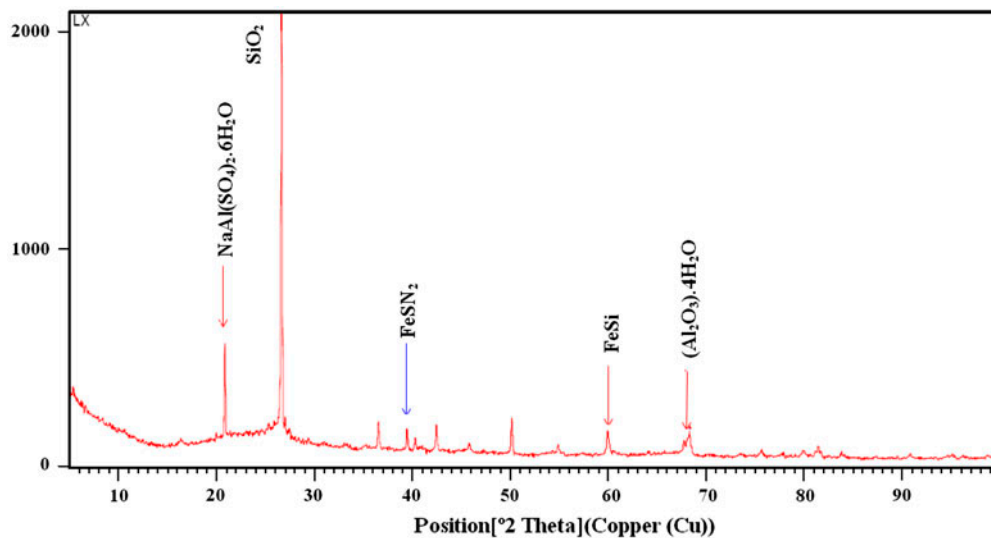


Fig. 2. XRD pattern of ACC.

The effect of m_{ad} value of ACC on the amount of TA adsorbed was also studied in range of $5 \leq m_{ad} \leq 25$ g/l at $pH_{i-opt} = 3.0$, while $C_o = 100$ mg/l, $T = 303$, and $t = 7$ h. As the m_{ad} value was increased, the adsorption of TA onto ACC first increased rapidly and it then became constant. TA removal efficiency was found to be 65.15% at $m_{ad} = 15$ g/l. For $m_{ad} > 15$ g/l, TA removal very minutely increased and becomes stable at 66%. Therefore, considering the cost of ACC, optimum m_{ad} (m_{ad-opt}) was taken as 15 g/l for further study. Adsorption depends on both concentration of adsorbate and available sites for adsorption. Increase in TA removal with the increase in m_{ad} values can be credited to availability of greater surface area and the more adsorption sites. For $m_{ad} \geq m_{ad-opt}$, TA removal efficiency depends principally on the concentration of the solution, not on the surface available [18].

Fig. 4 shows the FTIR spectra of blank and TA loaded ACC. FTIR spectra of blank ACC show sharp and high peaks at $\sim 1,085$, ~ 795 , and ~ 461 cm^{-1} . Peak at $\sim 1,085$ cm^{-1} may indicate the existence of Alcohols, Ethers, Carboxylic Acids, and Esters. Presence of the phenyl ring has their vibrations at ~ 795 cm^{-1} .

TA loaded ACC FTIR spectra explains shifted and changed peak height indicating that the functional groups at these wave numbers are involved in the TA adsorption. TA loaded ACC FTIR spectra shows some additional peaks at $\sim 3,853$, $\sim 3,745$, $\sim 3,615$, $\sim 3,419$, and $\sim 3,204$ cm^{-1} which correspond to phenols confirming TA adsorption. The adsorption peaks at $3,420$ cm^{-1} are ascribed to the vibrations of water molecules [19]. Peak $\sim 1,600$ cm^{-1} has been observed in both loaded and blank ACC due to C=C stretching absorption [20].

3.3. Adsorption kinetics and controlling mechanism

Fig. 5 shows the effect of contact time of adsorbent (ACC) with adsorbate (TA) by data points for $C_o = 50$ – 200 mg/l, $pH_{i-opt} = 3$, $m_{ad-opt} = 15$ g/l, and $t = 7$ h. It can be seen that TA adsorption reaches to equilibrium value after 1, 4, and 5 h for C_o values of 50, 100, and 200 mg/l, respectively. This increasing equilibrium time with C_o conclude that TA adsorption on to ACC is limited by TA concentration.

To investigate the kinetics of adsorption pseudo-first-order and pseudo-second-order kinetic models were studied.

Pseudo-first-order model is given as [21]:

$$q_t = q_e[1 - \exp(-k_f t)] \quad (3)$$

where q_t is TA adsorbed (mg/g) at time (t) (min) and k_f is the rate constant of pseudo first-order adsorption (min^{-1}).

Pseudo-second-order model is represented as [22,23]:

$$q_t = \frac{tk_s q_e^2}{1 + tk_s q_e} \quad (4)$$

The initial adsorption rate, h (mg/g min), at $t \rightarrow 0$ is defined as,

$$h = k_s q_e^2 \quad (5)$$

where k_s is the rate constant (g/mg min).

Kinetic experimental adsorption data were fitted to these two kinetic models using nonlinear regression fit. Marquardt's percent standard deviation (MPSD) error function was used to evaluate error [24]. The best-fit estimated parameters values of the model, correlation coefficients, and MPSD values are given in Table 2. R^2 values are higher (0.91, 0.97, and 0.98) for pseudo-second-order kinetic model in comparison to pseudo-first-order kinetic model (0.78, 0.95, and 0.96). Also, MPSD values are lower for pseudo-second-order kinetic model. These data confirms that the pseudo-second-order kinetic model best-fit the adsorption kinetics of TA on to ACC. The fitting of pseudo-second-order model with kinetic experimental data is shown in Fig. 5 by solid line. The value of q_e was found to increase with an increase in C_o , whereas, k_s decreased with an increase in C_o (Table 2), indicating kinetics is limited by TA concentration.

Since the adsorption process was assured good mixing with ACC and high concentration of TA, therefore, it may be possible that the intraparticle pore diffusion is the rate-controlling step during the adsorption process [25]. Intraparticle diffusion model proposed by Weber and Morris [26] was studied for this purpose, which is expressed by following equation:

$$q_t = k_{id} t^{1/2} + I \quad (6)$$

where k_{id} is the intraparticle diffusion rate constant (mg/g $min^{1/2}$) and I is the intercept representing thickness of the boundary layer. Higher value of intercept explains thicker boundary layer [18]. Plot of q_t vs. $t^{1/2}$ should be linear and passed through origin, if intraparticle pore diffusion is rate controlling, if not, intercept is measure of boundary layer thickness [27]. If data shows multi-linear plots, adsorption process is controlled by two or more steps.

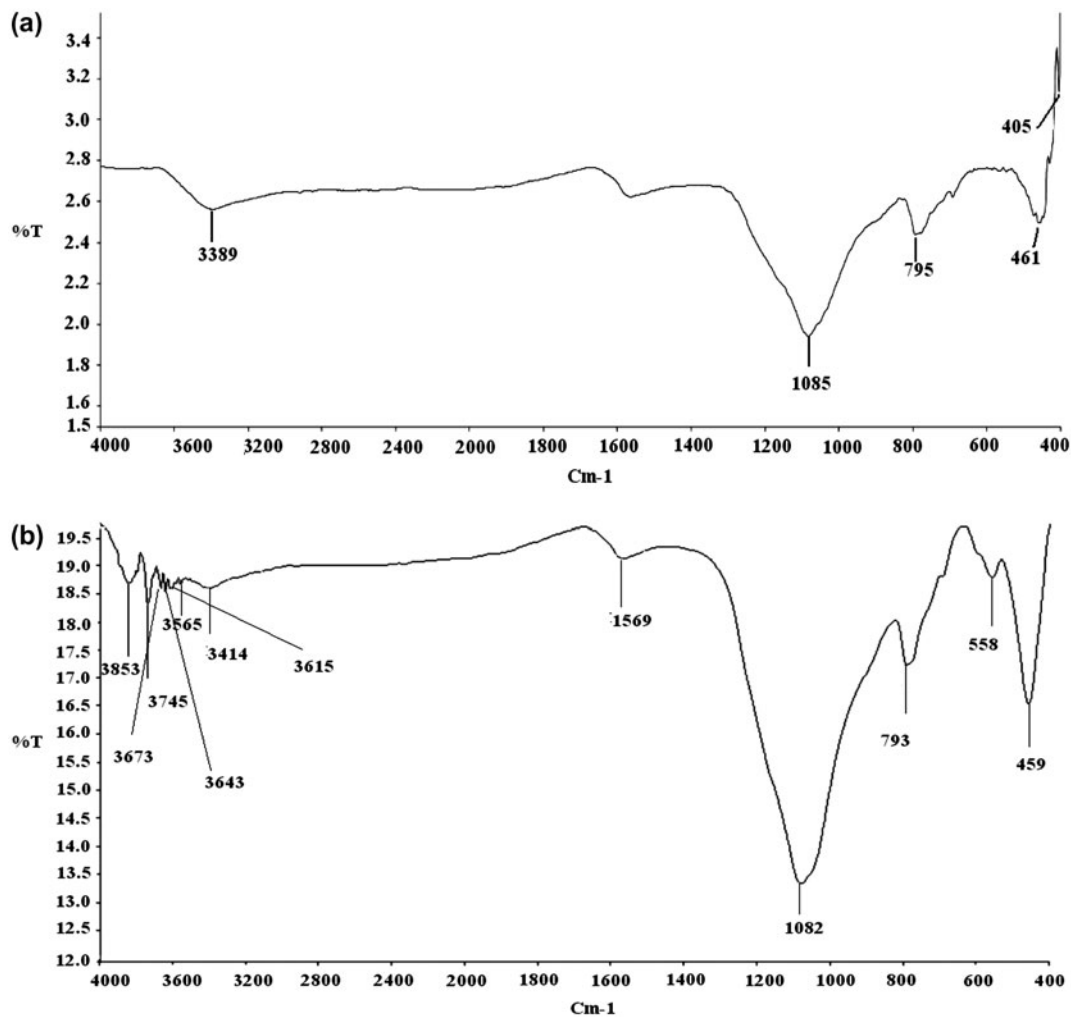


Fig. 4. FTIR spectra of (a) blank and (b) tannic acid loaded ACC.

Fig. 6 shows a representative q_t vs. $t^{0.5}$ plot for adsorption onto ACC for $C_0=200, 100$ and 50 mg/l at 301 K, $pH_{i-opt}=3$ and $m_{ad-opt}=15$ g/l. Two linear plots were found, which indicate more than one process is controlling the adsorption. The first portion is attributed to the slow equilibrium stage with intra-particle diffusion dominating, and second linear portion is the final equilibrium stage where intra-particle diffusion is very slow due to the extremely low residual TA concentration in the solution.

Slopes of first linear portions ($k_{id,1}$) are higher for higher C_0 , (Table 2) which shows an accelerated diffusion of TA through meso-pores due to greater driving force at higher C_0 . Also, deviation of straight lines from the origin indicates that the both surface adsorption and intra-particle transport within the pores of ACC controls the TA adsorption onto ACC.

3.4. Adsorption isotherm modelling and thermodynamics

To study the correlation between the amount of the adsorbate adsorbed (q_e) with concentration in the aqueous phase (C_e) at equilibrium, various isotherm models were used to validate the experimental data. For this TA adsorption onto ACC was studied at different T ranging from 291 – 311 K with $C_0=50$ – 200 mg/l, $pH_{i-opt}=3$, $m_{ad-opt}=15$ g/l and $t=7$ h. TA adsorption onto ACC was found to increased with an increase in T concluding that TA adsorption onto ACC is endothermic (Fig. 7). This increased capacity of ACC at higher temperature may be due to activation of the ACC surface and/or creation of new active sites on the adsorbent surface [17]. This could be due to degree of penetration within ACC structure overcoming the activation energy barrier and enhancing the rate of intraparticle diffusion [18,28].

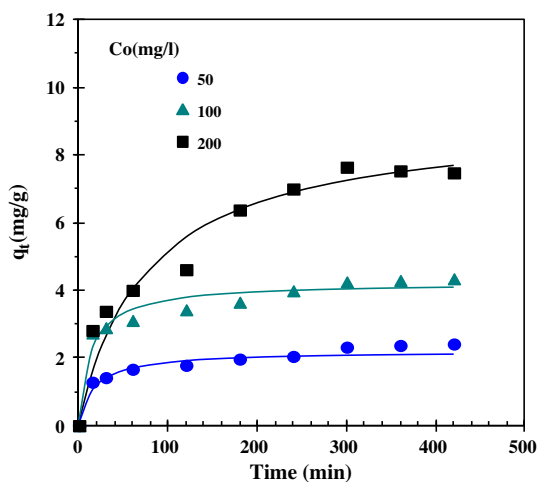


Fig. 5. Effect of contact time on the TA removal by ACC. Experimental data points given by the symbols and the lines predicted by the pseudo-second-order model. $T = 301\text{ K}$, $m_{\text{ad-opt}} = 15\text{ g/l}$.

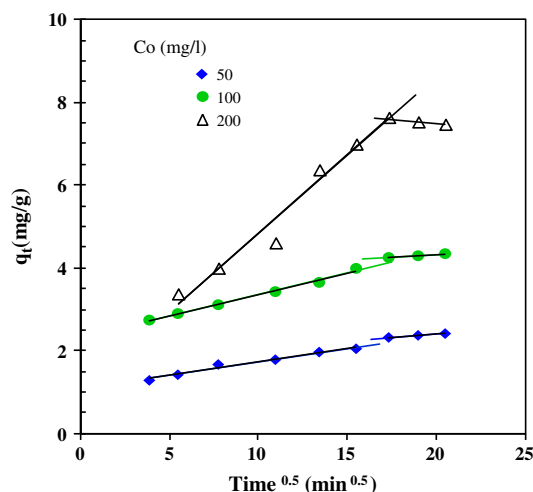


Fig. 6. Weber-Morris plot for the TA removal by ACC. $t = 7\text{ h}$, $C_0 = 50\text{--}200\text{ mg/l}$, and $m_{\text{ad-opt}} = 15\text{ g/l}$.

Langmuir [29], Temkin [30], and Redlich and Peterson (R-P) [31] isotherms were used to validate the isothermal equilibrium experimental data using non-linear regression fit. Table 3 shows the values of R^2 and various other isotherm parameters associated with various isotherms (Langmuir, Temkin and R-P isotherms) fitting to the experimental data. It may be seen that, there are marginal difference in R^2 values for different isotherms. Therefore, any of the isotherms can be used for isotherm modeling. But generally, it may be concluded that R-P isotherm best-fits the equilibrium adsorption of TA onto ACC at all

temperatures. The validation of various isotherms studied with experimental data points is shown in Fig. 7 by solid lines. q_m was found to increase with increase in temperature showing higher affinity to adsorbent at higher temperature and endothermic nature of adsorption of TA on to ACC.

To study the thermodynamics of adsorption of TA on to ACC, Gibbs free energy change, ΔG° (kJ/mol), change in enthalpy, ΔH° (kJ/mol), entropy change, ΔS° (J/mol K) and equilibrium adsorption constant (K) were calculated from classical thermodynamics equation of the adsorption process [32]:

Table 2

Kinetic parameters for the TA removal by ACC ($t = 7\text{ h}$, $C_0 = 50\text{--}200\text{ mg/l}$, and $m_{\text{ad-opt}} = 15\text{ g/l}$)

<i>Pseudo-first-order model</i>						
C_0 (mg/l)	$q_{e,\text{exp}}$ (mg/g)	$q_{e,\text{calc}}$ (mg/g)	k_f (min^{-1})	R^2	MPSD	
200	7.341	7.344	0.013	0.96	25.54	
100	4.343	3.783	0.048	0.95	24.60	
50	2.547	1.967	0.043	0.78	28.20	
<i>Pseudo-second-order model</i>						
C_0 (mg/l)	$q_{e,\text{calc}}$ (mg/g)	k_s (g/mg min)	h (mg/g min)	R^2	MPSD	
200	9.092	0.001	0.119	0.97	19.32	
100	4.220	0.017	0.303	0.97	15.82	
50	2.199	0.025	0.123	0.91	17.11	
<i>Intra-particle diffusion</i>						
C_0 (mg/l)	$k_{\text{id},1}$ (mg/g $\text{min}^{1/2}$)	I_1 (mg/g)	R^2	$k_{\text{id},2}$ (mg/g $\text{min}^{1/2}$)	I_2 (mg/g)	R^2
200	0.386	0.99	0.96	0.126	9.92	1
100	0.103	2.32	0.992	0.0292	3.74	0.995
50	0.0649	1.07	0.974	0.0294	1.81	0.999

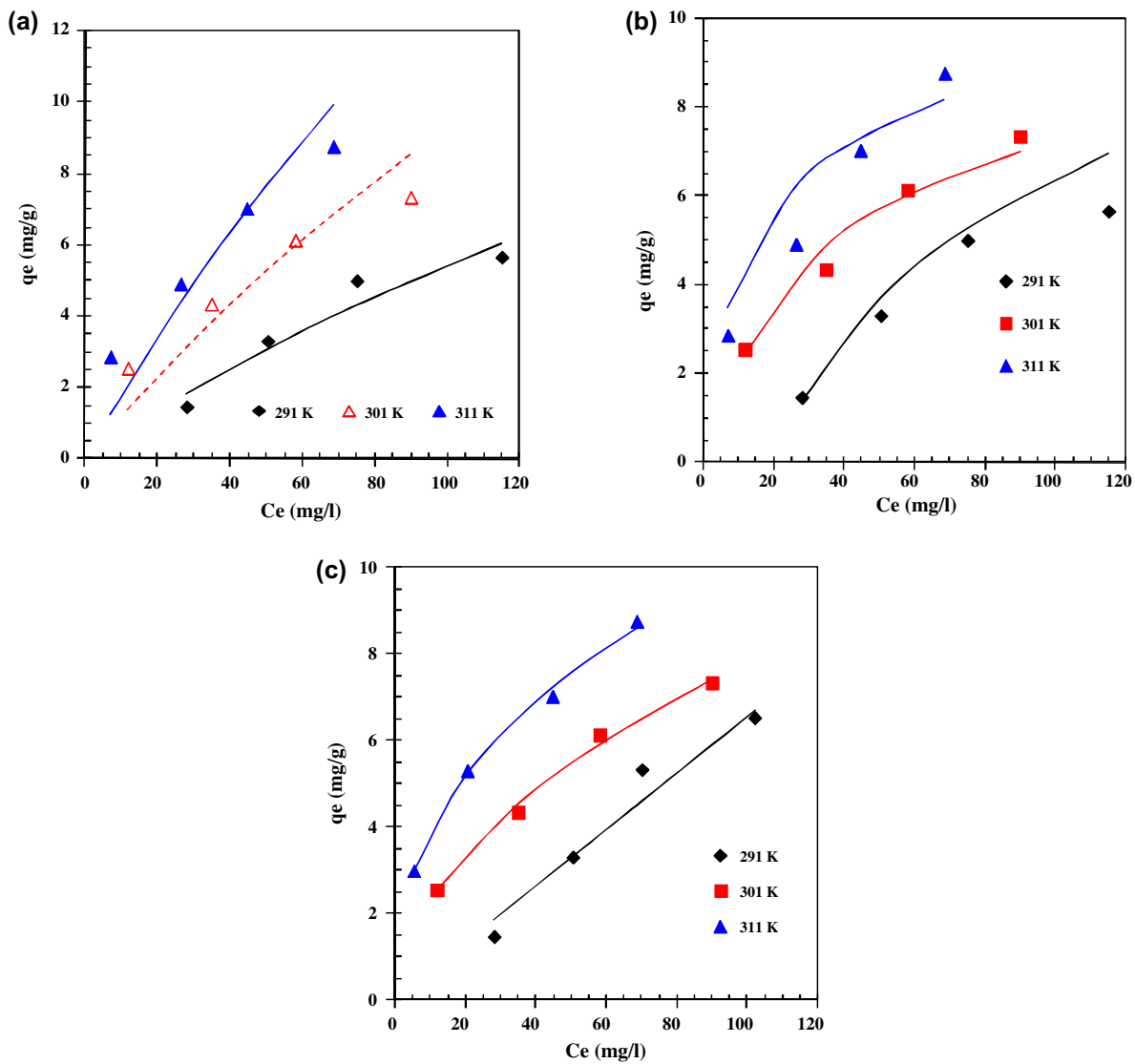


Fig. 7. Equilibrium adsorption isotherms at different temperature for the treatment of TA by ACC. Experimental data points given by symbols and the lines predicted by (a) Langmuir isotherm, (b) Temkin isotherm and (c) R-P isotherm model. $t = 7$ h, $C_o = 50$ – 200 mg/l, and $m_{ad-opt} = 15$ g/l.

$$\ln K = \frac{-\Delta G_0}{RT} = \frac{\Delta S_0}{RT} - \frac{\Delta H_0}{R} \frac{1}{T} \quad (7)$$

where T is the absolute temperature (K), R is the universal gas constant (8.314×10^{-3} kJ mol $^{-1}$ K $^{-1}$) and K ($= q_e/C_e$) is the single point or linear sorption distribution coefficient.

ΔH_0 and ΔS° can be found from linear van't Hoff plot ($\ln K$ vs. T^{-1}) (Fig. 8). Thermodynamic parameters obtained are shown in Table 3. Positive value of ΔH° confirms the endothermic nature of TA adsorption on to ACC. Positive value of ΔS° shows the affinity of ACC to TA molecules [33] and the negative value of ΔG° advocates that the adsorption process is

feasible and spontaneous without any induction period [13]. Generally the value of ΔG° for physisorption is between -20 and 0.0 kJ/mol, and that for chemisorption is between -400 and -80 kJ/mol [34]. Value of ΔG° in this study indicates that TA adsorption on to ACC is physisorption.

3.5. Regeneration of ACC

Two methods, solvent desorption and thermal desorption were studied for desorption of TA from ACC [35,36]. Solvent desorption study was performed by shaking 250 mL conical flasks containing 50 mL of aqueous solutions of 0.1N of C_2H_5OH , acetone

Table 3

Isotherm and thermodynamics parameters for the removal of TA removal by ACC ($t=7\text{h}$, $C_o=50\text{--}200\text{mg/l}$, and $m_{\text{ad-opt}}=15\text{g/l}$)

Isotherms	Parameters	Temperature (K)		
		291	301	311
Langmuir $q_e = \frac{q_m K_L C_e}{1 + K_L C_e}$	K_L (L/mg)	0.0027	0.003	0.0038
	q_m (mg/g)	25.428	40	47.9
	R^2	0.962	0.995	0.998
Temkin $q_e = B_T \ln(K_T C_e)$	B_1	3.924	2.254	2.053
	K_T (L/mg)	0.051	0.248	0.779
	R^2	0.988	0.985	0.967
Redlich–Peterson $q_e = \frac{K_R C_e}{1 + a_R C_e^\beta}$	a_R (L/mg)	0.00	2.6476	9.4584
	K_R (L/mg)	0.066	2.144	15.141
	β	0.00	0.499	0.600
	R^2	0.95	0.998	0.99
Thermodynamics parameters				
$K \times 10^{-3}$ (l/kg)		68.04	231.59	735.269
ΔG_0 (kJ/mol)		−10.21	−13.63	−17.07
ΔH_0 (kJ/mol)		89.55		
ΔS_0 (kJ/mol K)		342.79		

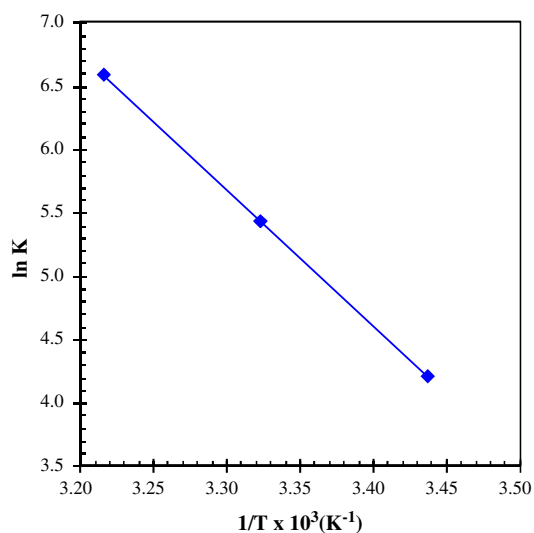


Fig. 8. Van't Hoff plot of adsorption equilibrium constant.

$(\text{CH}_3)_2\text{CO}$, and NaOH at 301 K for 24 h in the orbital incubator shaker with separated TA loaded ACC from TA solution after adsorption [35]. For thermal desorption study, dried TA loaded ACC (at 378 K for 2 h) was placed in a muffle furnace at 623 K and after 4 h the samples were taken from the furnace and kept in the desiccator.

After solvent and thermal desorption process, the ACC was again used as adsorbent for removal of TA at $C_o=100\text{mg/l}$ and 301 K. This adsorption–desorption cycle was repeated five times.

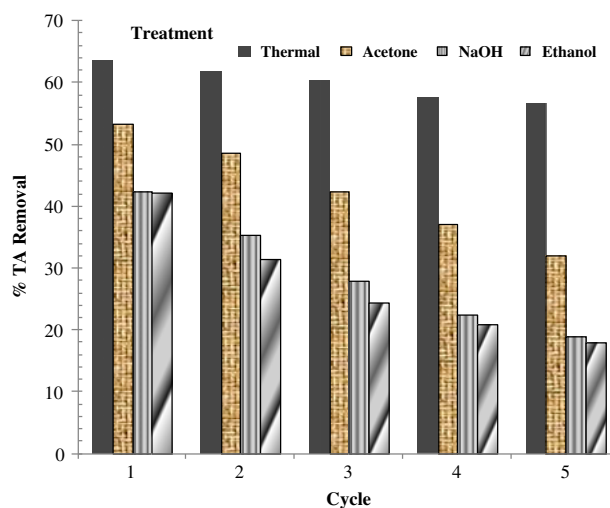


Fig. 9. TA removal efficiency of ACC after various desorption–adsorption cycles with Heat, Acetone, NaOH, and Ethanol.

Fig. 9 shows the TA removal efficiency of ACC after five desorption–adsorption cycles. In solvent desorption study, least desorption of TA was observed with the NaOH and ethanol which is nearly same, and acetone showed maximum desorption of TA from ACC. It can also be seen in Table 4 that q_e value decreased from 3.56 to 2.14, 2.83 to 1.26, and 2.82 to 1.2 mg/g (for cycles 1–5) for acetone, NaOH and ethanol, respectively. Therefore, ACC can be

Table 4
 q_e (mg/g) values of ACC after various adsorption-desorption cycles ($C_0 = 100$ mg/l, and $m_{ad-opt} = 15$ g/l)

Desorption method	q_e (mg/g)				
	Adsorption–desorption cycle				
	1	2	3	4	5
Heat treatment	4.23	4.12	4.03	3.84	3.77
Acetone	3.56	3.25	2.83	2.48	2.14
NaOH	2.83	2.36	1.86	1.49	1.26
Ethanol	2.82	2.10	1.62	1.40	1.20

reused for several times for adsorption of TA followed by desorption with acetone effectively giving 32.1% TA removal efficiency.

In thermal desorption study, thermally desorbed ACC from TA was again used for adsorption of TA at $C_0 = 100$ mg/l, $m_{ad} = 15$ g/l, $T = 301$ K, and $t = 7$ h. Once again, TA-loaded ACC was exposed to thermal desorption by the same procedure. This adsorption-desorption cycle was repeated five times and results are shown in Fig. 9. From cycles 1–5, q_e value decreased from 4.23–3.77 mg/g (Table 4) giving 56.6% TA removal efficiency after fifth adsorption-desorption cycle, which is maximum. Therefore, it can be concluded that thermal desorption method is more efficient than solvent desorption for TA from ACC, and ACC can be reused many times with effective TA removal efficiency.

4. Conclusion

Intra-particle diffusion study indicated that the both surface adsorption and intra-particle transport within the pores of ACC controls the TA adsorption onto ACC. TA adsorption study at various temperatures showed increased capacity of ACC at increased temperature indicating TA adsorption onto ACC is endothermic. q_m was found to increase with increase in temperature showing higher affinity to adsorbent at higher temperature.

Solvent desorption study showed least desorption of TA with NaOH and ethanol, and, acetone showed maximum desorption. Thermal desorption method was found more efficient than solvent desorption for TA from ACC; and ACC can be reused many times with effective TA removal efficiency.

References

- [1] J.H. An, S. Dultz, Adsorption of tannic acid on chitosan-montmorillonite as a function of pH and surface charge properties, *Appl. Clay Sci.* 36 (2007) 256–264.
- [2] J. Wang, C. Zheng, S. Ding, H. Ma, Y. Ji, Behaviours and mechanisms of tannic acid adsorption on an amino-functionalized magnetic nano-adsorbent, *Desalination* 273 (2011) 285–291.
- [3] J. Wang, A. Li, L. Xu, Y. Zhou, Adsorption of tannic and gallic acids on a new polymeric adsorbent and the effect of Cu(II) on their removal, *J. Hazard. Mater.* 169 (2009) 794–800.
- [4] J. Wang, S. Zheng, J. Liu, Z. Xu, Tannic acid adsorption on amino-functionalized magnetic mesoporous silica, *Chem. Eng. J.* 165 (2010) 10–16.
- [5] W.W. Li, X.D. Li, K.M. Zeng, Aerobic biodegradation kinetics of tannic acid in activated sludge system, *Biochem. Eng. J.* 43 (2009) 142–148.
- [6] J. Lin, Y. Zhan, Z. Zhu, Y. Xing, Adsorption of tannic acid from aqueous solution onto surfactant-modified zeolite, *J. Hazard. Mater.* 193 (2011) 102–111.
- [7] J. Wang, A. Li, L. Xu, Y. Zhou, Adsorption studies of tannic acid by commercial ester resin XAD-7, *Chin. J. Poly. Sci.* 28(2) (2010) 231–239.
- [8] J.P. Kushwaha, V.C. Srivastava, I.D. Mall, Treatment of dairy wastewater by inorganic coagulants: Parametric and disposal studies, *Water Res.* 44(20) (2010) 5867–5874.
- [9] M.Y. Chang, R.S. Juang, Adsorption of tannic acid, humic acid, and dyes from water using the composite of chitosan and activated clay, *J. Colloid Interface Sci.* 278 (2004) 18–25.
- [10] V. Vinod, T. Anirudhan, Sorption of tannic acid on zirconium pillared clay, *J. Chem. Technol. Biotechnol.* 77 (2002) 92–101.
- [11] C. Moreno-Castilla, M.V. López-Ramón, L.M. Pastrana-Martínez, M.A. Álvarez-Merino, M.A. Fontecha-Cámara, Competitive adsorption of the herbicide fluoxypyr and tannic acid from distilled and tap water on activated carbons and their thermal desorption, *Adsorption* 18 (2012) 173–179.
- [12] T. Anirudhan, M. Ramachandran, Adsorptive removal of tannin from aqueous solutions by cationic surfactant-modified bentonite clay, *J. Colloid Interface Sci.* 299 (2006) 116–124.
- [13] C. Sarıclı-Özdemir, Y. Önal, Equilibrium, kinetic and thermodynamic adsorptions of the environmental pollutant tannic acid onto activated carbon, *Desalination* 251 (2010) 146–152.
- [14] F. Liu, Z. Guo, S. Zheng, Z. Xu, Adsorption of tannic acid and phenol on mesoporous carbon activated by CO₂, *Chem. Eng. J.* 183 (2012) 244–252.
- [15] E. Chibowski, M. Espinosa-Jimenez, A. Ontiveros-Ortega, E. Giménez-Martín, Surface free energy, adsorption and zeta potential in leacril/tannic acid system, *Langmuir* 14 (1998) 5237–5244.
- [16] Z. Ryu, J. Zheng, M. Wang, B. Zhang, Characterization of pore size distributions on carbonaceous adsorbents by DFT, *Carbon* 37 (1999) 1257–1264.
- [17] D. Rameshraj, V.C. Srivastava, J.P. Kushwaha, I.D. Mall, Quinoline adsorption onto granular activated carbon and bagasse fly ash, *Chem. Eng. J.* 181–182 (2012) 343–351.
- [18] J.P. Kushwaha, V.C. Srivastava, I.D. Mall, Treatment of dairy wastewater by commercial activated carbon and bagasse fly ash: Parametric, kinetic and equilibrium modelling, disposal studies, *Bioresour. Technol.* 101(10) (2010) 3474–3483.
- [19] S. Tie, H. Lee, Y. Bae, M. Kim, K. Lee, C. Lee, Monodisperse Fe₃O₄/Fe@SiO₂ core/shell nanoparticles with enhanced magnetic property, *Colloids Surf. Physicochem. Eng. Aspects* 293 (2007) 278–285.
- [20] M. Jung, K. Ahn, Y. Lee, K. Kim, J. Rhee, J.T. Park, K. Paeng, Adsorption characteristics of phenol and chlorophenols on granular activated carbon (ACC), *Microchem. J.* 70 (2001) 123–131.
- [21] P.K. Malik, Use of activated carbons prepared from sawdust and rice-husk for adsorption of acid dyes: A case study of Acid yellow 36, *Dyes Pigm.* 56 (2003) 239–249.
- [22] Y.S. Ho, G. McKay, Sorption of dye from aqueous solution by peat, *Chem. Eng. J.* 70 (1998) 115–124.

- [23] Y.S. Ho, G. McKay, Pseudo-second order model for adsorption processes, *Process Biochem.* 34 (1999) 451–465.
- [24] D.W. Marquardt, An algorithm for least-squares estimation of nonlinear parameters, *J. Soc. Ind. Appl. Math.* 11 (1963) 431–441.
- [25] R. Aravindhan, J.R. Rao, B.U. Nair, Removal of basic yellow dye from aqueous solution by adsorption on green algae: *Caulerpa scalpelliformis*, *J. Hazard. Mater.* 142 (2007) 68–76.
- [26] W.J. Weber, Jr., J.C. Morris, Kinetics of adsorption on carbon from solution, *J. Sanitary Eng. Div., ASCE* 89 (1963) 31–59.
- [27] O. Gercel, A. Ozcan, A.S. Ozcan, H.F. Gercel, Preparation of activated carbon from a renewable bio-plant of *Euphorbia rigida* by H_2SO_4 activation and its adsorption behavior in aqueous solutions, *Appl. Surf. Sci.* 253 (2007) 4843–4852.
- [28] Z. Aksu, E. Kabasakal, Batch adsorption of 2,4-dichlorophenoxy-acetic acid (2,4-D) from aqueous solution by granular activated carbon, *Sep. Purif. Technol.* 35 (2004) 223–240.
- [29] I. Langmuir, The adsorption of gases on plane surfaces of glass, mica and platinum, *J. Am. Chem. Soc.* 40 (1918) 1361–1403.
- [30] M.I. Temkin, V. Pyzhev, Kinetics of ammonia synthesis on promoted iron catalysts, *Acta Phys. chim. URSS* 12 (1940) 327–356.
- [31] O. Redlich, D.L. Peterson, A useful adsorption isotherm, *J. Phys. Chem.* 63 (1959) 1024–1026.
- [32] V.C. Srivastava, I.D. Mall, I.M. Mishra, Multi-component adsorption study of metal ions onto bagasse fly ash using Taguchi's design of experimental methodology, *Ind. Eng. Chem. Res.* 46 (2007) 5697–5706.
- [33] Y. Onal, C. Akmil-Basar, D. Eren, C. Saric-Ozdemir, T. Depci, Adsorption kinetics of malachite green onto activated carbon prepared from tunçbilek lignite, *J. Hazard. Mater.* B128 (2006) 150–157.
- [34] Q.S. Liu, T. Zheng, P. Wang, J.P. Jiang, N. Li, Adsorption isotherm, kinetic and mechanism studies of some substituted phenols on activated carbon fibers, *Chem. Eng. J.* 157 (2010) 348–356.
- [35] M.S. Rauthula, V.C. Srivastava, Studies on adsorption/desorption of nitrobenzene and humic acid onto/from activated carbon, *Chem. Eng. J.* 168 (2011) 35–43.
- [36] S. Suresh, V.C. Srivastava, I.M. Mishra, Isotherm, thermodynamics, desorption and disposal study for the adsorption of catechol and resorcinol onto granular activated carbon, *J. Chem. Eng. Data* 56(4) (2011) 811–818.